

TextCenGen: Attention-Guided Text-Centric Background Adaptation for Text-to-Image Generation

Tianyi Liang¹, Jiangqi Liu¹, Sicheng Song¹, Shiqi Jiang¹, Shenzhuo Zhang¹, Yifei Huang¹, Changbo Wang¹, Chenhui Li¹

¹East China Normal University
chli@cs.ecnu.edu.cn

Abstract

Recent advancements in Text-to-image (T2I) generation have witnessed a shift from adapting text to fixed backgrounds to creating images around text. Traditional approaches are often limited to generate layouts within static images for effective text placement. Our proposed approach, **TextCenGen**, introduces a dynamic adaptation of the space region for text-friendly image generation, focusing on **text-centric** design and visual harmony **generation**. Our method employs force-directed attention guidance in T2I models to generate images that strategically reserve whitespace for pre-defined text areas, even for text or icons at the golden ratio. Observing how cross-attention maps affect object placement, we detect and repel conflicting objects using a force-directed graph approach, combined with a spatial excluding cross-attention constraint for smooth attention in whitespace areas. As a novel task in graphic design, experiments indicate that *TextCenGen* outperforms existing methods with more harmonious compositions. Furthermore, our method significantly enhances T2I model outcomes on our specially collected prompt datasets, catering to different text positions. These results demonstrate the efficacy of *TextCenGen* in creating more harmonious and integrated text-image compositions.

1 Introduction

In graphic design, achieving an effective synergy between text and imagery is essential for clear communication. The choice of background can greatly influence text visibility and comprehension. A common design objective is to place text within an image in a way that is both visually pleasing and communicatively clear. A preferred strategy is to position the text in the golden ratio, which is believed to be aesthetically optimal (see Figure 2a). However, designers often grapple with the issue of backgrounds that compete with or obscure the text, as illustrated in Figure 2b, where unsuitable backgrounds detract from the text’s readability and aesthetic appeal, regardless of any adjustments to text color or size. We aim to facilitate the creation of text-friendly images (see Figure 2c), ideal for

text placement and catering to the growing demand due to increasing use of Text-to-Image (T2I) models for background graphics.

Traditional approaches to graphic design, especially in poster creation, have largely focused on arranging layouts with natural background images, elements, and text [Guo *et al.*, 2021; Cao *et al.*, 2012; O’Donovan *et al.*, 2014; Li *et al.*, 2022]. However, producing text-friendly images remains a significant challenge due to the complexity of background elements. Our insight, derived from Figure 2c, reveals that a clear separation between the main objects and the text areas is essential. Recent advancements in diffusion-related research have shown that it is possible to manipulate the primary objects within cross-attention maps, making the adaptation of background images to accommodate text a feasible endeavor [Hertz *et al.*, 2022; Epstein *et al.*, 2023].

In response, we introduce **TextCenGen**, as illustrated in Figure 1, a novel method that employs cross-attention maps and force-directed graphs for effective object placement and whitespace optimization. We also implement a spatial excluding cross-attention constraint to ensure smooth attention in areas designated for text. To establish a new benchmark for this innovative task, we constructed a diverse dataset gathered from three unique sources, along with three distinct evaluation metrics, to comprehensively assess the performance. The contributions of our paper are three-fold:

- We propose a novel task of text-friendly text-to-image generation, which creates images that satisfy both the prompt and reserve space for pre-defined text placements. Our benchmark includes a specialized dataset and tailored evaluation metrics designed to rigorously assess this novel challenge.
- We introduce **TextCenGen**, a plug-and-play, training-free framework. This approach allows for dynamic placement of text at user-specified location within an image, with the image being generated or adapted to accommodate the text.
- Our prominent module, the force-directed cross-attention guidance, is an effective addition to the denoising process in T2I models. This module strategically directs cross-attention map within the image generation process, ensuring harmonious layout of text and imagery.

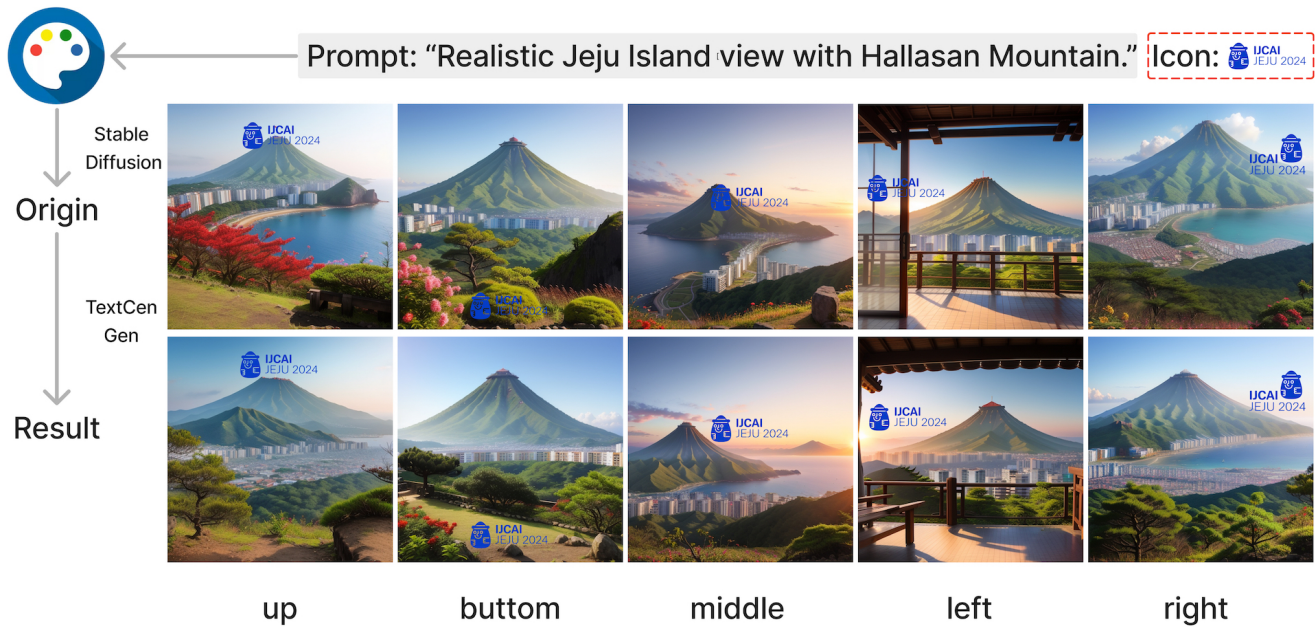


Figure 1: TextCenGen is a training-free method designed to generate text-friendly images. It simultaneously generates the original and result images. During the denoising process of the original image, the generation of the result image is guided based on the encroachment into the planned space regions in the original. This approach ensures sufficient blank space at specific positions, typically where text or icons are centered, in the result image.

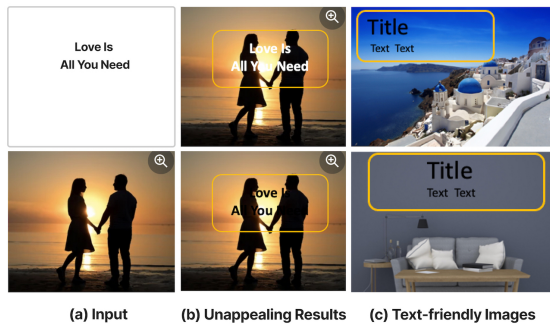


Figure 2: Our target text-friendly images. (a) An input layout for text at the golden ratio, intended as a Valentine’s Day card on a selected background image. (b) shows background interference causing unappealing text visibility, and (c) presents standard text-friendly image adaptation with clear text integration.

2 Related Work

Text Layout of Natural Images has evolved significantly, transitioning from traditional layout designs to more advanced methods influenced by deep learning. Initially, poster design focused on creating layouts with given background images, elements, and text [Guo *et al.*, 2021; Cao *et al.*, 2012; O’Donovan *et al.*, 2014; Li *et al.*, 2022]. The integration of deep learning in text layout of natural image generation has led to various models such as GAN [Goodfellow *et al.*, 2014; Zheng *et al.*, 2019; Li *et al.*, 2019; Zhou *et al.*, 2022], VAE [Jyothi *et al.*, 2019], transformers [Vaswani *et al.*, 2017; Inoue *et al.*, 2023b; Wang *et al.*, 2023] and diffusion models [Ho *et al.*, 2020; Hui *et al.*, 2023; Inoue *et al.*, 2023a;

Chai *et al.*, 2023; Li *et al.*, 2023a]. These models have been instrumental in learning layout patterns from large datasets. Subsequent research explored methods to retrieve matching background images based on text and image description [Jin *et al.*, 2022]. Since the development of image editing method based on diffusion model, scene text generation methods such as TextDiffuser [Chen *et al.*, 2023b; Chen *et al.*, 2023a] and DiffText [Zhang *et al.*, 2023a] have addressed the challenges of generating clear text with diffusion models. However, these methods often rely on the presence of a ‘sign’ or similar element within the prompt (e.g., a T-shirt) to place text. They do not explicitly tackle the problem of creating text-friendly images where the background itself is crafted to adapt pre-defined text regions. Our approach, *TextCenGen*, significantly extends these capabilities by allowing the primary objects in generated images to yield space to text regions, resulting in more harmonious and aesthetically pleasing compositions.

Text-to-Image Generation has advanced with diffusion models [Ho *et al.*, 2020], producing realistic images and videos that align closely with text prompts [Rombach *et al.*, 2022; Singer *et al.*, 2023; Chen *et al.*, 2023c]. Innovations in this field include GLIDE [Nichol *et al.*, 2022], which integrates text conditions into the diffusion process, DALL-E 2 [Ramesh *et al.*, 2022] with its diffusion prior module for high-resolution images, and Imagen [Saharia *et al.*, 2022], which uses a large T5 language model to enhance semantic representation. Stable diffusion [Rombach *et al.*, 2022] projects images into latent space for diffusion processing. Beyond text conditions, the manipulation of diffusion models through image-level conditions has been explored. Methods

such as image inpainting [Balaji *et al.*, 2022] aim to generate coherent parts of an image, while SDG [Liu *et al.*, 2023] introduces semantic inputs to guide unconditional DDPM sampling. In addition, techniques such as [Meng *et al.*, 2021] use images as editing conditions in denoising processes. Scene text generation methods such as TextDiffuser [Chen *et al.*, 2023b; Chen *et al.*, 2023a] and GlyphDraw [Ma *et al.*, 2023] have also emerged, utilizing textual layouts or masks to guide text generation in images. These advancements represent the growing versatility and potential of T2I models in diverse applications.

Attention Guided Image Editing has emerged as a critical solution to the challenge of translating human preferences and intentions into visual content through text descriptions. These approaches, as seen in works like [Li *et al.*, 2023c; Avrahami *et al.*, 2023; Zhang *et al.*, 2023b; Zhao *et al.*, 2023], involve learning auxiliary modules on paired data. However, a significant limitation of these training-based methods is the substantial cost and effort required for repeated training for different control signals, model architectures, and checkpoints. In response to these challenges, training-free techniques have emerged, using the inherent weights of attention and the characteristics of pre-trained models to control the characteristics of objects such as size, shape, appearance, and location [Hertz *et al.*, 2022; Epstein *et al.*, 2023; Patashnik *et al.*, 2023; Xie *et al.*, 2023]. These methods typically utilize basic conditions, such as bounding boxes, for precise control over object positioning and scene composition [Mo *et al.*, 2023]. Our approach takes this further by applying force-directed graph techniques to cross-attention map edits, allowing for more automated and precise object transformations in T2I editing.

3 Method

3.1 Overview

Given an input text region R and a prompt T_{prompt} , our framework aims to generate a text-friendly image I_{res} . Specifically, the output image has (1) reduced overlap between the primary object and R , (2) sufficient smoothness and minimal color variation in R , and (3) the image still fits the prompt. Our framework is shown in Figure 3.

Initially, we consider the k^{th} token of T_{prompt} , which corresponds to the cross-attention map A_k . Some methods utilize A_k to locate and edit objects within generated images [Epstein *et al.*, 2023]. In response to our first concern, we analyze the denoising process of an unguided image (I_{ori}) from a given prompt. We establish the subset of tokens (O) that refer to objects that need modification. The conflict detector operates based on the average attention intensity shared between the shapes of objects corresponding to A_k and R in an overlapping manner. For every token $k \in O$, we introduce *Force-Directed Cross-Attention Guidance* for moving objects. In this scheme, objects are treated as centroid vertex within a graph, with a sequence of forces being applied (see Figure 4) to adjust object positions.

For the second consideration, we employ strategies derived from recent technologies that limit the range of the attention map [Zhang *et al.*, 2023a]. Consequently, we propose a *spatial excluding cross-attention constraint* to prevent an extensive attention density from encroaching on R .

We find that repulsive force often moves required objects out of the image. Addressing the third concern, our denoising process incorporates a loss function with additional regularization terms to safeguard the shapes and positions of other objects. To prevent objects from being dislocated outside limits while retaining their reasonable shapes, we also introduce the notions of *Margin Force* $F_m()$ and *Warping Force* $F_w()$.

3.2 Force-Directed Cross-Attention Guidance

Cross-Attention and Centroid of Object. To seamlessly integrate the concept of force-directed graphs into the loss guidance of the denoising process in latent diffusion models, we delve into the extraction and manipulation of attention maps and activations. We use softmax normalized attention matrices $\mathcal{A}_{i,t} \in \mathbb{R}^{H_i \times W_i \times K}$ extracted from the standard denoising forward step $\epsilon_{\theta_i}(z_i; t, y)$. This enables us to manipulate the control over objects referred to in the text conditioning y at distinct indices k , by adjusting the related attention channel(s) $\mathcal{A}_{i,t,\dots,k} \in \mathbb{R}^{H_i \times W_i \times |k|}$. The centroid of the attention map is a two-dimensional vector, defined by the equation: 1

$$\text{centroid}(k) = \frac{1}{\sum_{h,w} \mathcal{A}_{h,w,k}} \left[\begin{array}{c} \sum_{h,w} h \mathcal{A}_{h,w,k} \\ \sum_{h,w} w \mathcal{A}_{h,w,k} \end{array} \right]. \quad (1)$$

To ensure the efficacy of our centroid-based object representation method, we initially assume that all objects are convex sets, adhering to the mathematical definition that for every pair of points within the object, the line segment connecting them lies entirely within the object. This assumption allows us to treat the extracted centroid (k) as vertices v_k in a graph, which are then subjected to force-directed attention guidance. Indeed, it is important to clarify that while each token k associated with \mathcal{A}_k appears as a single entity in Figure 3, it actually represents an average of \mathcal{A}_k^l across all layers l in the U-Net architecture. Practically, our method is applied individually to each layer, ensuring a nuanced and layer-specific approach to force-directed attention guidance.

Layer-wise Conflict Multi-Target Detector. To effectively manage conflicts between text and objects in our images, we have developed a layer-wise conflict multi-target detector, denoted as $D()$. This detector is crucial for identifying tokens k within each layer l of the U-Net that correspond to objects that require modifications in relation to text regions. The detector function $D(k, R, A_k^l)$ operates as follows:

$$D(k, R, A_k^l) = \begin{cases} 1, & \text{if } \text{mean}(\mathcal{A}_{h,w,k}^l \cap R) > \theta \\ 0, & \text{otherwise} \end{cases} \quad (2)$$

where $\mathcal{A}_{h,w,k}^l$ is the attention map for token k at layer l , and R is the region designated for text. The function returns a value of 1 when the mean attention within the overlap between $\mathcal{A}_{h,w,k}^l$ and R exceeds a predefined threshold θ , indicating a conflict that requires our guidance function. Identifying and adjusting the bounding boxes is visualized in Figure 3.

Repulsive Force. The fundamental repulsive force $F_{rep}(v_i, v_j) = \frac{-\xi^2}{\|pos(v_i) - pos(v_j)\|}$, ensures that each element is placed separately. ξ denotes the general strength of the force, while $p(v_i)$ and $p(t/o)$ indicate the positions of the

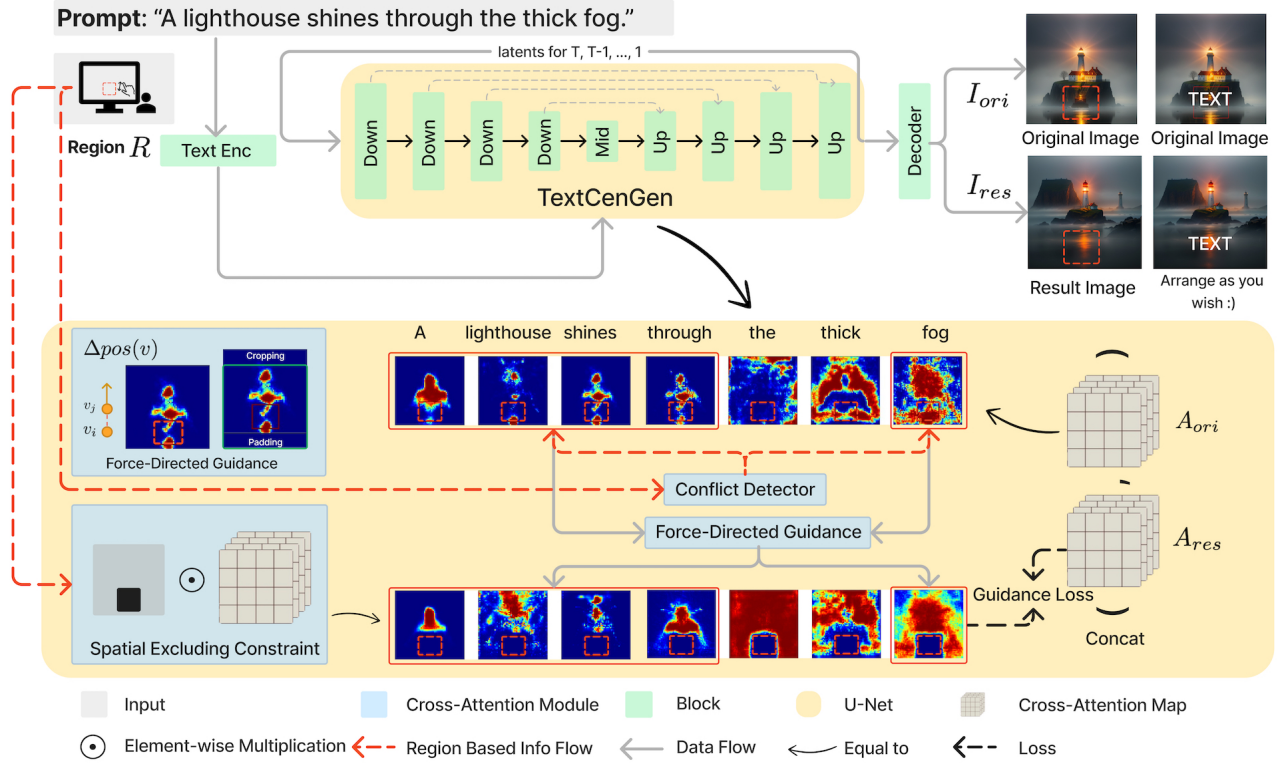


Figure 3: In our approach, the model receives a blank region (R) denoted as red-dotted area, and a text prompt as its inputs. The prompt is then used concurrently in a Text-to-Image (T2I) model to generate both an original image and a result image. During each step of the diffusion model’s denoising process, the cross-attention map from the U-Net associated with the original image is used to direct the denoising of the result image in the form of a loss function. Throughout this procedure, a conflict detector identifies objects that could potentially conflict with R . To mitigate such conflicts, a force-directed graph method is applied to spatially repel these objects, ensuring that the area reserved for the text prompt remains unoccupied. To further enhance the smoothness of the attention mechanism, a spatial excluding cross-attention constraint is integrated into the cross-attention map.

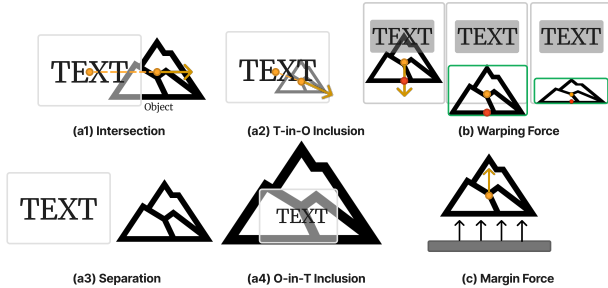


Figure 4: Illustration of four set relationships and their associated forces. The *Repulsive Force* separates object and text centroids during intersections (a1) and enclosures (a2). The *Margin Force* (b) and *Warping Force* (c) prevent boundary overstepping. Details on text exclusion within object regions (a4) are discussed in the ‘Excluding Cross-Attention Constraint’ section.

vertex and the target object, respectively. For scenarios that encompass multiple targets, our framework adopts a cumulative force approach to balance attention across these

elements. This is quantified by the formula:

$$F_{multi-tar}(v_i) = \sum_{j=1}^n \omega_j \cdot \frac{-\xi^2}{\|p(v_i) - p(tar_j)\|}, \quad (3)$$

where ω_j are coefficients for balancing attention across targets. To regulate the impact of these forces and avoid excessive dominance by any single target, we introduce a force balance constant α in the form of $\frac{F_{rep}}{\alpha + F_{rep}}$. α ensures that the forces exerted do not exceed a practical threshold, thereby maintaining visual equilibrium in complex scenes (shown in Figure 5).

Margin Force. The Margin Force is a critical component of our force-directed graph algorithm, designed to prevent significant vertices from being expelled from visual boundaries. This force, $F_m(v) = \frac{-m}{d(v, border)^2}$, is activated as a vertex v approaches the edge of the display area, typically a delineated rectangular space. The force is directed inward to ensure that crucial vertices remain within the designated visual region. The constant m modulates the force’s intensity, and $d(v, border)$ represents the distance of the vertex v from the nearest boundary (see Figure 4).

Displacement and Position Update. To compute the total displacement $\Delta pos(v)$, we sum the repulsive and mar-

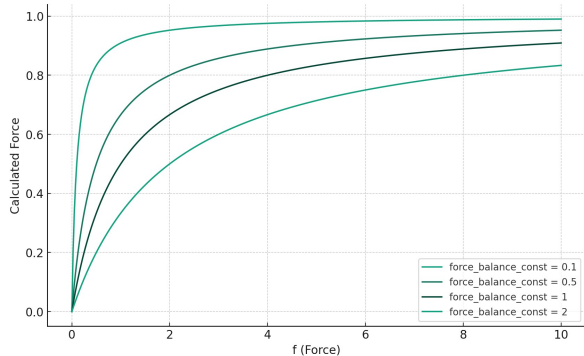


Figure 5: Influence of the force balance constant. The graph illustrates the effects of four different values for α on F_{rep} versus the final force. The curves reveal that as α increases, the rate of convergence to the limit progresses more rapidly.

gin forces together: $\Delta pos(v) = F_{rep}(v) + F_m(v)$ Subsequently, we update the vertex’s position as follows: $pos(v) = pos(v) + \Delta pos(v)$. For the attention map \mathcal{A}_k^l , this update is applied as a whole, with excess regions outside the boundaries being discarded and the remaining areas filled with zeros. But this method introduces the risk of the object being moved out of the boundaries and then being discarded, so it is necessary to introduce the following ‘warping force’ to prevent this from happening.

Warping Force. In addressing the dynamics of our force-directed graph algorithm, particularly for the movement of cross-attention maps \mathcal{A}_k^l in each layer, we employ affine transformations as a pivotal mechanism. This approach facilitates the comprehensive translation and scaling of the entire map, preserving the relative positions within the image domain. Initially, we delineate our visual area or image space as a $H \times W$ two-dimensional array A . Within this canvas A , we identify a key region, the object O , defined by the coordinates (x, y, a, b) , where (x, y) marks the upper-left corner and (a, b) the lower-right corner. The movement (move) is calculated based on the sum of repulsive force $F_{rep}(v)$ and margin force $F_m(v)$, yielding the total displacement $\Delta pos(v) = F_{rep}(v) + F_m(v)$. Applying $\Delta pos(v)$ to both A and O , we obtain the transformed canvas A' and the object O' . Subsequently, we shift our coordinate system’s origin to a vertex within A' that remains within the canvas boundaries, establishing a new origin O_{new} . This repositioning is crucial when O' exceeds the visual boundaries of A . In such cases, we scale the moved \mathcal{A}_k^l to ensure that the bounding box of O' fits precisely within the confines of \mathcal{A}_k^l . Scaling factors S_x and S_y , are calculated as $S_x = \min(1, \frac{H-1}{a'})$ and $S_y = \min(1, \frac{W-1}{b'})$, where (a', b') are the new coordinates of O' . Finally, the scaled \mathcal{A}_k^l and O' are reverted back to their original coordinate origin (see the warping force in Figure 4). A critical aspect of our approach is the transformation of the reference frame. After displacing O due to $\Delta pos(v)$, a new reference frame is established, centered at O_{new} . The coordinates of O in this new frame are calculated as $(x_{new}, y_{new}) = (x + \Delta x - O_{new_x}, y + \Delta y - O_{new_y})$. The affine transformation, considering this frame shift, is represented as:

$$\mathbf{T} = \begin{pmatrix} S_x & 0 & \Delta x - O_{new_x} \\ 0 & S_y & \Delta y - O_{new_y} \\ 0 & 0 & 1 \end{pmatrix}. \quad (4)$$

This matrix transforms the coordinates of O , ensuring that it remains visible within A after transformation. This carefully planned process secures the region O within A , even after dynamic changes. It upholds the structure of the cross-attention map and the core principles of our force-directed graph algorithm, balancing key vertices visibility and graph fluidity.

3.3 Spatial Excluding Cross-Attention Constraint

Our goal is to maintain a smooth background in the text region denoted as R . As illustrated in Figure 3, during each timestep of the forward pass in the diffusion model, we modify the cross-attention maps at every layer. The cross-attention map is represented as $\mathcal{A}_k^l \in \mathbb{R}^{H \times W \times K}$, where $H \times W$ are the dimensions of A^l at different scales, and K signifies the maximum token length at layer l . The set I consists of indices of tokens corresponding to areas outside the text in the prompt. We resize R to align with the HW dimensions. Subsequently, a new cross-attention map for each layer l is computed as $\mathcal{A}_{k,new}^l = \{\lambda \times \mathcal{A}_k^l \odot (1 - R) \mid \forall k \in O\}$, where O represents the tokens needing editing. This procedure effectively redirects the model’s attention away from R , ensuring that the background in this region remains undisturbed and visually smooth. This spatially exclusive approach enhances the clarity and coherence of the generated images, particularly in areas designated for text insertion.

The final loss function of our denoising process is defined as:

$$\mathcal{L} = \|\mathcal{A}_{ori} - \mathcal{A}_{res}\|^2 + \gamma \mathcal{L}_{norm}. \quad (5)$$

In this case, \mathcal{A}_{ori} and \mathcal{A}_{res} stand for the original and altered versions of matrix A , correspondingly, while $\|\cdot\|$ signifies the Euclidean distance among these cross-attention maps. Furthermore, the inclusion of the regularization term $\gamma \mathcal{L}_{norm}$ derived from self-guidance[Epstein *et al.*, 2023], strives to prevent overfitting, where γ denotes a delicately selected weighting parameter intended to maintain a balance in the impact of the norm penalty, \mathcal{L}_{norm} , within the aggregate loss function \mathcal{L} .

4 Experiments

Our evaluation strategy is designed to thoroughly assess the effectiveness of TextCenGen in generating text-centric images. The evaluation is structured into quantitative and qualitative analyses, alongside an ablation study to understand the contribution of individual components of our model.

4.1 Implementation Details

Experimental Settings. Our model is built with Diffusers. The pre-trained models are stable-diffusion-v1-5. While generating, the size of the output images is 512×512 . We use one A6000 and ten A40 GPUs for evaluation. Detailed parameter settings are provided in the appendix.

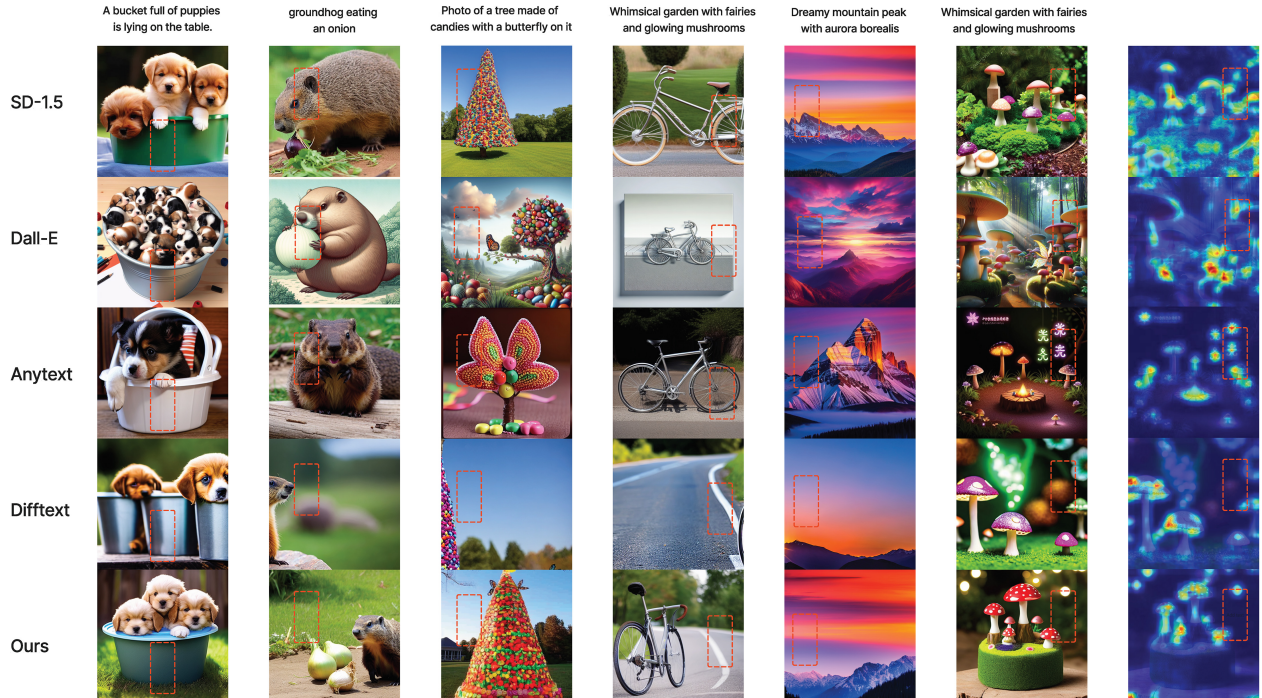


Figure 6: The results of comparison. Each column showcases six varied prompts, the final column depicting the saliency map of the result image generated from the mushroom prompt. The red-dotted area denotes the target area preserved for either text or icon images.

Dataset for Evaluation Our evaluation contains 27,000 images generated from 2,700 unique prompts, each tested in ten different random region R . The dataset combined synthesized prompts generated by ChatGPT, and 700 prompts from the Prompt2Prompt template ([Hertz *et al.*, 2022]) designed for attention guidance, focusing on specific objects and their spatial relationships. Additionally, we included 1,000 DiffusionDB prompts ([Wang *et al.*, 2022]), chosen for their real-world complexity. This diverse and comprehensive dataset, spanning synthetic to user-generated prompts, provided a broad test ground to evaluate the efficacy of our *TextCenGen* method in various T2I scenarios.

4.2 Comparison with Existing Methods

We compared *TextCenGen* with several potential models to evaluate its efficiency. The baseline models include: Native Stable Diffusion [Rombach *et al.*, 2022], Dall-E 3 [Ramesh *et al.*, 2022], AnyText [Tuo *et al.*, 2023] and DiffText [Zhang *et al.*, 2023a]. Dall-E uses the prompt "text-friendly in the position" to specify the region R . Similar to AnyText and DiffText, we chose to randomly generate several masks in a fixed pattern across the map to simulate regions need to be edited. More detail can be found in appendix.

Metrics and Quantitative Analysis. To evaluate model performance, we used metrics assessing various aspects of the generated images. The CLIP Score [Hessel *et al.*, 2021; Huang *et al.*, 2021; Radford *et al.*, 2021; cli, 2022] measured semantic fidelity, ensuring images align with textual

descriptions. The total variation (TV) loss [Rudin and Osher, 1994] assessed the visual coherence and smoothness of the background in relation to text region R , which is crucial for harmonious compositions. Saliency Map Intersection Over Union (IOU) quantified focus and clarity around text areas. We propose the Visual-Textual Concordance Metric (VTCM) that combines a global metric increasing with value (CLIP Score) and local metrics that benefit from lower values (Saliency IOU and TV Loss) within R . The VTCM formula is:

$$VTCM = \text{CLIP Score} \times \left(\frac{1}{\text{Saliency IOU}} + \frac{1}{\text{TV Loss}} \right). \quad (6)$$

Our quantitative analysis in Table 1 shows that our method, **TextCenGen**, outperforms native stable diffusion 1.5, especially in background smoothness and saliency harmony, even surpassing the latest Dalle-3. Notably, despite DiffText achieving the best results in terms of background significance as represented by the Saliency IOU and the region smoothness (TV loss), its CLIP score, which measures semantic similarity, significantly lags behind other methods. Scene text rendering often blurs text locations, unlike our approach of moving main objects to create space. Our method results in more natural and harmonious text layouts with highest VTCM.

Qualitative Analysis. Our qualitative analysis, shown in Figure 6, involved a comparison across different models using prompts and positions within the same quadrant. Dall-E 3, which relies solely on text inputs, exhibited significant variability and could not consistently clear the necessary areas for

Dataset	Metrics	Stable Diffusion	Dall-E 3	AnyText	DiffText	Ours
P2P Template	CLIP Score \uparrow	28.26	25.73	27.94	17.67	27.96
	Saliency IOU \downarrow	29.89	52.64	54.34	21.30	28.37
	TV Loss \downarrow	14.11	18.02	22.55	9.10	13.29
	VTCM \uparrow	2.95	1.92	1.75	2.77	3.09
DiffuisonDB	CLIP Score \uparrow	27.84	25.80	26.80	17.92	27.20
	Saliency IOU \downarrow	30.11	56.82	55.88	23.49	27.80
	TV Loss \downarrow	12.30	21.16	20.39	8.86	11.55
	VTCM \uparrow	2.73	1.98	1.79	2.41	2.76
Synthetics Prompt	CLIP Score \uparrow	28.45	26.20	27.43	18.78	28.10
	Saliency IOU \downarrow	31.42	51.52	53.24	24.00	30.83
	TV Loss \downarrow	15.61	17.85	21.46	11.56	15.17
	VTCM \uparrow	3.19	1.67	1.79	2.79	3.33

Table 1: Quantitative comparison of our method with other methods. Red indicates the best scores and blue marking the second best scores.

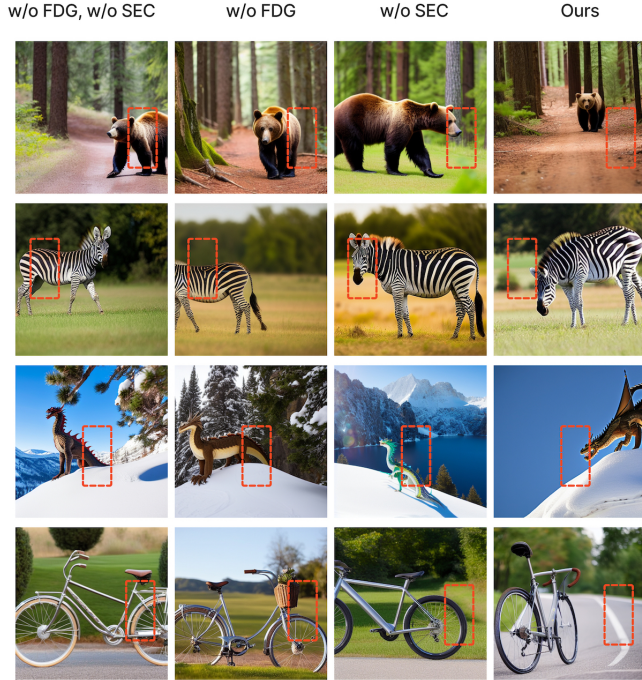


Figure 7: The results of ablation. We examine TextCenGen with or without the implementation of Force-Directed Cross-Attention Guidance (FDG) and Spatial Excluding Cross-Attention Constraint (SEC). The red-dotted area denotes the target area preserved for either text or icon images. Images produced with both FDG and SEC yield outcomes identical to those created using TextCenGen alone. Conversely, images created without FDG and SEC are comparable to those derived from the original stable diffusion model.

text. DiffText was effective in creating large blank spaces but often failed to fulfill the prompt accurately. For example, in the cases of 'bicycle' and 'canny tree', the central concepts were missing from the images. This probably occurs because the method reduces attention outside the region R , leading to a mismatch between the result image and the intended semantics of the prompt. Introducing text to images was tricky, as TV Loss showed, but TextCenGen kept object detail and background quality well. It shows that our force-directed method effectively balances text and visuals in images.

4.3 Ablation Study

Figure 7 presents the results of our ablation study. This study was designed to elucidate the individual contributions of the various components embedded within our proposed model. As part of our comprehensive analysis, we focused on assessing the two key factors: (1) the impact of the Force-Directed Cross-Attention Guidance, (2) the effectiveness of the Spatial Excluding Cross-Attention Constraint.

Impact of Force-Directed Cross-Attention Guidance.

Our model's force-directed feature is key to gently shifting where objects are placed. Without this, we might just bluntly edit the cross-attention map, which could mess up important parts of the picture. This part of our model helps us make sure we don't ruin the image structure by harshly removing attention map from areas.

Effects of Spatial Excluding Cross-Attention Constraint.

Despite successful relocation of conflict object-related tokens, spaces left behind may not inherently lead to a well-blended transition. Our experimental results underscore that the integration of the Spatial Excluding Cross-Attention Constraint greatly improve the smoothness of the remaining image sections.

5 Conclusion

We present TextCenGen, a novel shift in T2I generation. This model abandons the traditional method of adapting text to pre-defined images for a more flexible, text-focused approach. TextCenGen modifies images to adapt text, employing force-directed cross-attention guidance to arrange whitespace. Furthermore, we have integrated a system to identify and relocate conflicting objects and a spatial exclusion cross-attention constraint for low saliency in whitespace areas.

Our approach has certain limitations. The force-directed cross-attention guidance, assuming convexity and centering on object centroids, may not be suitable for non-convex shapes. This could lead to reduced size or fragmentation of objects. Future work will address these challenges to improve the quality of the output images. Additionally, we observed the generation of unintended objects in blank areas not mentioned in the original prompts. Future work could use BLIP-2 [Li *et al.*, 2023b] to update image prompts and detect new conflict objects.

References

- [Avrahami *et al.*, 2023] Omri Avrahami, Thomas Hayes, Oran Gafni, Sonal Gupta, Yaniv Taigman, Devi Parikh, Dani Lischinski, Ohad Fried, and Xi Yin. Spatext: Spatio-textual representation for controllable image generation. In *CVPR*, pages 18370–18380, 2023.
- [Balaji *et al.*, 2022] Yogesh Balaji, Seungjun Nah, Xun Huang, Arash Vahdat, Jiaming Song, Karsten Kreis, Miika Aittala, Timo Aila, Samuli Laine, Bryan Catanzaro, et al. ediffi: Text-to-image diffusion models with an ensemble of expert denoisers. *arXiv preprint arXiv:2211.01324*, 2022.
- [Cao *et al.*, 2012] Ying Cao, Antoni B Chan, and Rynson WH Lau. Automatic stylistic manga layout. *ACM Transactions on Graphics*, 31(6):1–10, 2012.
- [Chai *et al.*, 2023] Shang Chai, Liansheng Zhuang, and Fengying Yan. Layoutdm: Transformer-based diffusion model for layout generation. In *CVPR*, pages 18349–18358, 2023.
- [Chen *et al.*, 2023a] Jingye Chen, Yupan Huang, Tengchao Lv, Lei Cui, Qifeng Chen, and Furu Wei. Textdiffuser-2: Unleashing the power of language models for text rendering. *arXiv preprint arXiv:2311.16465*, 2023.
- [Chen *et al.*, 2023b] Jingye Chen, Yupan Huang, Tengchao Lv, Lei Cui, Qifeng Chen, and Furu Wei. Textdiffuser: Diffusion models as text painters. *arXiv preprint arXiv:2305.10855*, 2023.
- [Chen *et al.*, 2023c] Xinyuan Chen, Yaohui Wang, Lingjun Zhang, Shaobin Zhuang, Xin Ma, Jiashuo Yu, Yali Wang, Dahua Lin, Yu Qiao, and Ziwei Liu. Seine: Short-to-long video diffusion model for generative transition and prediction. *arXiv preprint arXiv:2310.20700*, 2023.
- [cli, 2022] Clipscore. <https://github.com/jmhessel/clipscore>, 2022.
- [Epstein *et al.*, 2023] Dave Epstein, Allan Jabri, Ben Poole, Alexei A. Efros, and Aleksander Holynski. Diffusion self-guidance for controllable image generation. *Advances in Neural Information Processing Systems*, 2023.
- [Goodfellow *et al.*, 2014] Ian Goodfellow, Jean Pouget-Abadie, Mehdi Mirza, Bing Xu, David Warde-Farley, Sherjil Ozair, Aaron Courville, and Yoshua Bengio. Generative adversarial nets. *Advances in neural information processing systems*, 27, 2014.
- [Guo *et al.*, 2021] Shunan Guo, Zhuochen Jin, Fuling Sun, Jingwen Li, Zhaorui Li, Yang Shi, and Nan Cao. Vinci: an intelligent graphic design system for generating advertising posters. In *CHI*, pages 1–17, 2021.
- [Hertz *et al.*, 2022] Amir Hertz, Ron Mokady, Jay Tenenbaum, Kfir Aberman, Yael Pritch, and Daniel Cohen-Or. Prompt-to-prompt image editing with cross attention control. *arXiv preprint arXiv:2208.01626*, 2022.
- [Hessel *et al.*, 2021] Jack Hessel, Ari Holtzman, Maxwell Forbes, Ronan Le Bras, and Yejin Choi. Clipscore: A reference-free evaluation metric for image captioning. In *EMNLP*, pages 7514–7528, 2021.
- [Ho *et al.*, 2020] Jonathan Ho, Ajay Jain, and Pieter Abbeel. Denoising diffusion probabilistic models. *Advances in neural information processing systems*, 33:6840–6851, 2020.
- [Huang *et al.*, 2021] Yupan Huang, Hongwei Xue, Bei Liu, and Yutong Lu. Unifying multimodal transformer for bi-directional image and text generation. In *ICML*, pages 1138–1147, 2021.
- [Hui *et al.*, 2023] Mude Hui, Zhizheng Zhang, Xiaoyi Zhang, Wenxuan Xie, Yuwang Wang, and Yan Lu. Unifying layout generation with a decoupled diffusion model. In *CVPR*, pages 1942–1951, 2023.
- [Inoue *et al.*, 2023a] Naoto Inoue, Kotaro Kikuchi, Edgar Simo-Serra, Mayu Otani, and Kota Yamaguchi. Layoutdm: Discrete diffusion model for controllable layout generation. In *CVPR*, pages 10167–10176, 2023.
- [Inoue *et al.*, 2023b] Naoto Inoue, Kotaro Kikuchi, Edgar Simo-Serra, Mayu Otani, and Kota Yamaguchi. Towards flexible multi-modal document models. In *CVPR*, pages 14287–14296, 2023.
- [Jin *et al.*, 2022] Chuhao Jin, Hongteng Xu, Ruihua Song, and Zhiwu Lu. Text2poster: Laying out stylized texts on retrieved images. In *ICASSP*, pages 4823–4827. IEEE, 2022.
- [Jyothi *et al.*, 2019] Akash Abdu Jyothi, Thibaut Durand, Jiawei He, Leonid Sigal, and Greg Mori. Layoutvae: Stochastic scene layout generation from a label set. In *ICCV*, pages 9895–9904, 2019.
- [Li *et al.*, 2019] Jianan Li, Jimei Yang, Aaron Hertzmann, Jianming Zhang, and Tingfa Xu. Layoutgan: Generating graphic layouts with wireframe discriminators. In *International Conference on Learning Representations*, 2019.
- [Li *et al.*, 2022] Chenhui Li, Peiyang Zhang, and Changbo Wang. Harmonious textual layout generation over natural images via deep aesthetics learning. *IEEE Transactions on Multimedia*, 24:3416–3428, 2022.
- [Li *et al.*, 2023a] Fengheng Li, An Liu, Wei Feng, Honghe Zhu, Yaoyu Li, Zheng Zhang, Jingjing Lv, Xin Zhu, Junjie Shen, Zhangang Lin, and Jingping Shao. Relation-aware diffusion model for controllable poster layout generation. In *Proceedings of the 32nd ACM International Conference on Information and Knowledge Management*, page 1249–1258, 2023.
- [Li *et al.*, 2023b] Junnan Li, Dongxu Li, Silvio Savarese, and Steven Hoi. Blip-2: Bootstrapping language-image pre-training with frozen image encoders and large language models. *arXiv preprint arXiv:2301.12597*, 2023.
- [Li *et al.*, 2023c] Yuheng Li, Haotian Liu, Qingyang Wu, Fangzhou Mu, Jianwei Yang, Jianfeng Gao, Chunyuan Li, and Yong Jae Lee. Gligen: Open-set grounded text-to-image generation. In *CVPR*, pages 22511–22521, 2023.
- [Liu *et al.*, 2023] Xihui Liu, Dong Huk Park, Samaneh Azadi, Gong Zhang, Arman Chopikyan, Yuxiao Hu, Humphrey Shi, Anna Rohrbach, and Trevor Darrell. More control for free! image synthesis with semantic diffusion guidance. In *WACV*, pages 289–299, 2023.

- [Ma *et al.*, 2023] Jian Ma, Mingjun Zhao, Chen Chen, Ruichen Wang, Di Niu, Haonan Lu, and Xiaodong Lin. Glyphdraw: Learning to draw chinese characters in image synthesis models coherently. *arXiv preprint arXiv:2303.17870*, 2023.
- [Meng *et al.*, 2021] Chenlin Meng, Yutong He, Yang Song, Jiaming Song, Jiajun Wu, Jun-Yan Zhu, and Stefano Ermon. Sdedit: Guided image synthesis and editing with stochastic differential equations. *arXiv preprint arXiv:2108.01073*, 2021.
- [Mo *et al.*, 2023] Sicheng Mo, Fangzhou Mu, Kuan Heng Lin, Yanli Liu, Bochen Guan, Yin Li, and Bolei Zhou. Freecontrol: Training-free spatial control of any text-to-image diffusion model with any condition. *arXiv preprint arXiv:2312.07536*, 2023.
- [Nichol *et al.*, 2022] Alexander Quinn Nichol, Prafulla Dhariwal, Aditya Ramesh, Pranav Shyam, Pamela Mishkin, Bob McGrew, Ilya Sutskever, and Mark Chen. Glide: Towards photorealistic image generation and editing with text-guided diffusion models. In *ICML*, pages 16784–16804. PMLR, 2022.
- [O’Donovan *et al.*, 2014] Peter O’Donovan, Aseem Agarwala, and Aaron Hertzmann. Learning layouts for single-pagegraphic designs. *IEEE Transactions on Visualization and Computer Graphics*, 20:1200–1213, 2014.
- [Patashnik *et al.*, 2023] Or Patashnik, Daniel Garibi, Idan Azuri, Hadar Averbuch-Elor, and Daniel Cohen-Or. Localizing object-level shape variations with text-to-image diffusion models. In *ICCV*, 2023.
- [Radford *et al.*, 2021] Alec Radford, Jong Wook Kim, Chris Hallacy, Aditya Ramesh, Gabriel Goh, Sandhini Agarwal, Girish Sastry, Amanda Askell, Pamela Mishkin, Jack Clark, et al. Learning transferable visual models from natural language supervision. In *ICML*, pages 8748–8763. PMLR, 2021.
- [Ramesh *et al.*, 2022] Aditya Ramesh, Prafulla Dhariwal, Alex Nichol, Casey Chu, and Mark Chen. Hierarchical text-conditional image generation with clip latents. *arXiv preprint arXiv:2204.06125*, 2022.
- [Rombach *et al.*, 2022] Robin Rombach, Andreas Blattmann, Dominik Lorenz, Patrick Esser, and Björn Ommer. High-resolution image synthesis with latent diffusion models. In *CVPR*, pages 10684–10695, 2022.
- [Rudin and Osher, 1994] Leonid I Rudin and Stanley Osher. Total variation based image restoration with free local constraints. In *Proceedings of 1st international conference on image processing*, volume 1, pages 31–35. IEEE, 1994.
- [Saharia *et al.*, 2022] Chitwan Saharia, William Chan, Saurabh Saxena, Lala Li, Jay Whang, Emily L Denton, Kamyar Ghasemipour, Raphael Gontijo Lopes, Burcu Karagol Ayan, Tim Salimans, et al. Photorealistic text-to-image diffusion models with deep language understanding. *Advances in Neural Information Processing Systems*, 35:36479–36494, 2022.
- [Singer *et al.*, 2023] Uriel Singer, Adam Polyak, Thomas Hayes, Xi Yin, Jie An, Songyang Zhang, Qiyuan Hu, Harry Yang, Oron Ashual, Oran Gafni, Devi Parikh, Sonal Gupta, and Yaniv Taigman. Make-a-video: Text-to-video generation without text-video data. In *ICLR*, 2023.
- [Tuo *et al.*, 2023] Yuxiang Tuo, Wangmeng Xiang, Jun-Yan He, Yifeng Geng, and Xuansong Xie. Anytext: Multilingual visual text generation and editing. *arXiv preprint arXiv:2311.03054*, 2023.
- [Vaswani *et al.*, 2017] Ashish Vaswani, Noam Shazeer, Niki Parmar, Jakob Uszkoreit, Llion Jones, Aidan N Gomez, Łukasz Kaiser, and Illia Polosukhin. Attention is all you need. *Advances in neural information processing systems*, 30, 2017.
- [Wang *et al.*, 2022] Zijie J. Wang, Evan Montoya, David Munechika, Haoyang Yang, Benjamin Hoover, and Duen Horng Chau. DiffusionDB: A large-scale prompt gallery dataset for text-to-image generative models. *arXiv:2210.14896 [cs]*, 2022.
- [Wang *et al.*, 2023] Ruichen Wang, Zekang Chen, Chen Chen, Jian Ma, Haonan Lu, and Xiaodong Lin. Compositional text-to-image synthesis with attention map control of diffusion models. *arXiv preprint arXiv:2305.13921*, 2023.
- [Xie *et al.*, 2023] Jinheng Xie, Yuexiang Li, Yawen Huang, Haozhe Liu, Wentian Zhang, Yefeng Zheng, and Mike Zheng Shou. Boxdiff: Text-to-image synthesis with training-free box-constrained diffusion. In *ICCV*, pages 7452–7461, 2023.
- [Zhang *et al.*, 2023a] Lingjun Zhang, Xinyuan Chen, Yaohui Wang, Yue Lu, and Yu Qiao. Brush your text: Synthesize any scene text on images via diffusion model. 2023.
- [Zhang *et al.*, 2023b] Lvmin Zhang, Anyi Rao, and Maneesh Agrawala. Adding conditional control to text-to-image diffusion models. In *ICCV*, pages 3836–3847, 2023.
- [Zhao *et al.*, 2023] Shihao Zhao, Dongdong Chen, Yen-Chun Chen, Jianmin Bao, Shaozhe Hao, Lu Yuan, and Kwan-Yee K Wong. Uni-controlnet: All-in-one control to text-to-image diffusion models. *Advances in Neural Information Processing Systems*, 2023.
- [Zheng *et al.*, 2019] Xinru Zheng, Xiaotian Qiao, Ying Cao, and Rynson WH Lau. Content-aware generative modeling of graphic design layouts. *ACM Transactions on Graphics*, 38(4):1–15, 2019.
- [Zhou *et al.*, 2022] Min Zhou, Chenchen Xu, Ye Ma, Tiezheng Ge, Yuning Jiang, and Weiwei Xu. Composition-aware graphic layout gan for visual-textual presentation designs. In *Proceedings of the Thirty-First International Joint Conference on*, pages 4995–5001, 7 2022.